

A nanosecond regenerative Ti:Sapphire amplifier for the simultaneous generation of 940 nm and of 320 nm pulses

Vincenzo Talluto¹ · Thomas Blochowicz² · Thomas Walther¹ 

Received: 6 October 2015 / Accepted: 1 April 2016 / Published online: 29 April 2016
© Springer-Verlag Berlin Heidelberg 2016

Abstract Narrowband cw radiation at 940 and 960 nm is used to seed a Nd:YAG-pumped regenerative Ti:Sapphire amplifier. A Pockels cell traps a slice of the seed radiation inside the amplifier cavity, generating two synchronized pulses and releasing them after amplification. The total pulse energy is as high as 9 mJ at a pulse duration of 6.5 ns and a Fourier-transform-limited bandwidth. The timing jitter between the two pulses at the two wavelengths is less than ± 300 ps. The relative pulse energy can be controlled by the relative seed laser power. Up to 1 mJ pulse energy at 320 nm was achieved by third-harmonic generation.

1 Introduction

The generation of synchronized laser pulses is of great interest for pump-probe experiments [1], resonant ionization spectroscopy [2] or the generation of tunable near-IR laser radiation by difference-frequency mixing in nonlinear optical crystals [3]. A flashlamp-pumped regenerative amplifier operating at the gain peak of Ti:Sapphire was developed by some of us a couple of years ago [4]. However, this system had some severe drawbacks regarding the performance. The upper-state lifetime of Ti:Sapphire is relatively short, giving rise to the necessity of specialized circuits to fire the flashlamps. Furthermore, this requires rather long crystals in order to provide enough gain, in turn

leading to a rather poor transverse beam profile of the laser in Ref. [4]. Moreover, this laser was simultaneously operated at 761 and 789 nm, i.e. very close to the gain maximum of Ti:Sapphire. For our particular application, the operation wavelengths of 940 and 960 nm far off the gain maximum of Ti:Sapphire were needed, reducing the gain to roughly 45 % of its value at 800 nm. Thus, the optical components of the amplifier have to be carefully selected in order to suppress spontaneous emission processes leading to wavelength and energy instabilities as well as uncontrolled lasing and possible damage of the amplifier. In addition, good transverse beam quality was essential as one of the output wavelengths was to be converted into the UV range by third-harmonic generation (THG).

The laser system is part of an experiment investigating the triplet state solvation dynamics in supercooled liquids [5]. By employing a two-photon excitation scheme with 320 and 940 nm, we are aiming at improving the overall signal-to-noise ratio and extending the observable relaxation time window.

2 Experimental set-up

The complete set-up of the entire experiment is shown schematically in Fig. 1. The outputs of two home-built cw external-cavity diode lasers (ECDL) in Littrow configuration operating at 940 and 960 nm are individually coupled into polarization maintaining fibres acting as spatial filters. The fibre outputs are superimposed employing a steep-edge long-pass interference filter (LP). The seed intensity at the two wavelengths is individually adjusted by a combination of half-wave plates and polarizing beam splitters. The combined seed beams are directed through a Glan-laser polarizer (GL), a 45° Faraday rotator (FR) and a half-wave plate.

✉ Thomas Walther
thomas.walther@physik.tu-darmstadt.de

¹ Institute for Applied Physics, TU Darmstadt, Darmstadt, Germany

² Institute for Condensed Matter Physics, TU Darmstadt, Darmstadt, Germany

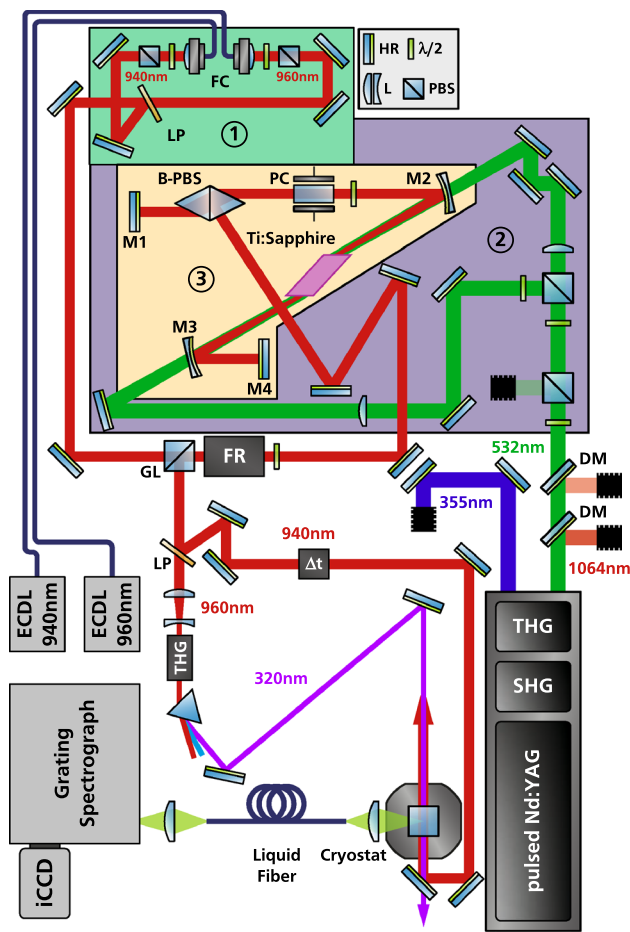


Fig. 1 Schematic drawing of the experiment. The *coloured areas* mark the seed superposition (1. *green*), pump beam (2. *blue*) and amplifier cavity (3. *yellow*). HR Highly reflective mirror, $\lambda/2$ Half-wave plate, L lens, PBS polarizing beam splitter, M1–M4: cavity mirrors, other abbreviations defined in text

The now s-polarized seed beams are then coupled into the amplifier cavity by a Brewster-cut polarizing beam splitter (B-PBS). Up to 50 mW of seed power at each wavelength is available inside the cavity.

The amplifier consists of a linear Z-resonator formed by four mirrors (M1–M4). M1 is a plane mirror with high reflectivity for both seed wavelengths. M2 and M3 are concave with a -10 m radius and have a high reflectivity for the seed wavelengths and a high transmission for the pump beam at 532 nm. Mirror M4 is plane and has a reflectivity of 99.8 % at 960 nm and 99 % at 940 nm, respectively. The coating is designed such that wavelengths below 930 nm are not reflected in order to suppress amplification of spontaneous emission (ASE) closer to the gain peak. In addition, it compensates for the gain difference of Ti:Sapphire between 940 and 960 nm. The Brewster-cut Ti:Sapphire rod with dimensions of $5 \times 5 \times 25$ mm³ is positioned between the curved mirrors.

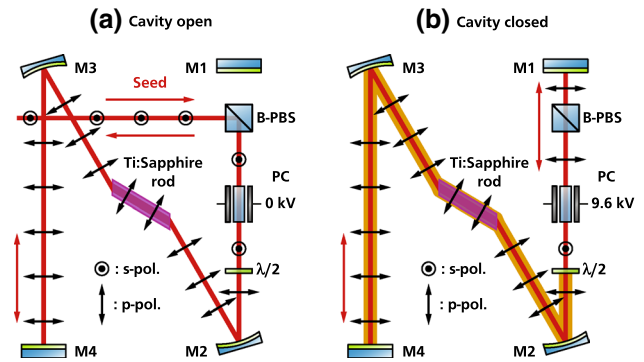


Fig. 2 Working principle of the regenerative amplifier cavity. In the open state (a), no voltage is applied to the Pockels cell, and the seed beam leaves the cavity before reaching mirror M1. By quickly setting the Pockels cell to its half-wave voltage of 9.6 kV, all the light between mirror M4 and the half-wave plate is trapped inside the cavity (b). After an integer number of round trips, the Pockels cell is turned off and the amplified pulses leave the cavity. The distance between M4 and the half-wave plate defines the pulse duration of the amplified pulses

A Pockels cell (PC, Lasermetrics 5046E) acting as a switchable half-wave plate is used to trap a small portion of the seed radiation inside the cavity once inversion is reached in the Ti:Sapphire medium by the pump pulse. Switching times of <4 ns are short compared to the round trip such that the trapped pulses are shorter than the round-trip time of the cavity, eliminating the formation of longitudinal modes. Thus, the seed radiation at the two wavelengths can be almost arbitrary combinations within the gain profile of the Ti:Sapphire crystal. After amplification of the pulses during several round trips in the cavity, the voltage on the PC is dropped again, leading to a cavity dump (see Fig. 2). A half-wave plate inside the cavity is employed to rotate the polarization into the plane of the laser resonator in order to minimize losses at the Ti:Sapphire crystal facets. Brewster-PBS, Faraday rotator and Glan-laser polarizer located outside the resonator act as an optical isolator separating the amplified pulses from the counter propagating seed.

The Ti:Sapphire crystal is pumped by the second harmonic of a flash-lamp pumped, pulsed Nd:YAG laser (Innolas Spitlight 600, RMS energy stability at 532 nm <1.3 %, flat-top beam profile, 6 mm diameter) with integrated second- and third-harmonic generation stages (SHG and THG) and a repetition rate of 10 Hz. The third harmonic at 355 nm can be used for measurements of the solvation dynamics as well. The second harmonic at 532 nm is separated from the residual radiation at 1064 nm by two short-pass dichroic mirrors (DM). The pulse energy of the pump is regulated by a half-wave plate and a polarizing beam splitter. The pump is then split into two beams and directed onto either facet of the Ti:Sapphire crystal.

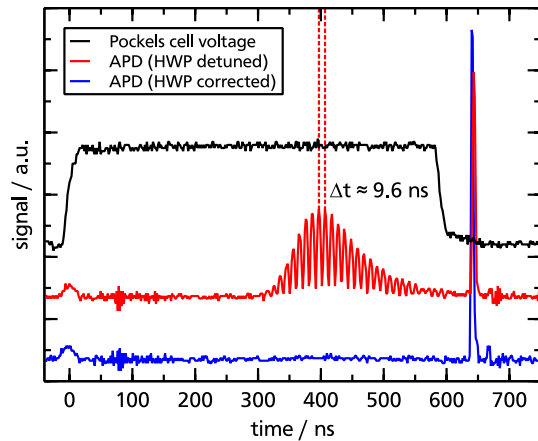


Fig. 3 Influence of half-wave plate detuning on the output of the amplifier. The Pockels cell voltage (*black curve*) was kept high longer than necessary to show the complete amplification process. In this case, the maximum amplification is reached after ≈ 400 ns. The small peak at 0 ns is caused by the pump pulse. Even though the timing of the Pockels cell is far from perfect a short pulse is visible after it is turned off. Please note that the additional delay of 50 ns between switching off the Pockels cell and detection of the pulse is due to the sum of the internal delay of the Pockels cell (40 ns) and the travel time difference between pump and output beam (10 ns)

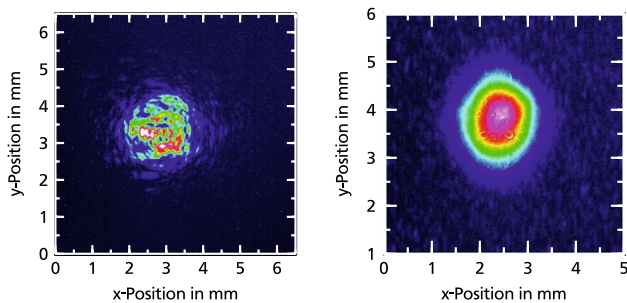


Fig. 4 Left: Pump beam profile 10 cm in front of the Ti:Sapphire crystal. Right: Beam profile of the output beam of the regenerative amplifier taken 50 cm after passing the Glan-laser polarizer. The concentric rings are artefacts caused by defects on the attenuator mounted in front of the CCD camera

Two plano-convex lenses with $f = +750$ mm are used to focus each pump beam (see Fig. 4). The foci are positioned behind the crystal to avoid laser-induced damage. Pulse duration at 1064 nm is specified as 6–7 ns. By delaying firing the Q-switch with respect to the flashlamps, the pulse duration was lengthened to 11.4 ns (FWHM) at 532 nm.

To avoid excessive losses during round trips inside the amplifier, the fast axis angle of the half-wave plate inside the cavity has to be carefully tuned. Therefore, a fast avalanche photo diode (APD, Laser components SAR500S3, 450 ps rise time) is used to observe the output of the amplifier. Figure 3 shows the APD signal recorded by a fast oscilloscope (Tektronix TDS5034B, 350 MHz bandwidth,

1.15 ns rise time, 20 ps/point). The signal with detuned half-wave plate (red curve) shows a strong modulation indicating the high losses at the B-PBS due to the wrong orientation of the polarization vector inside the cavity. The period of the modulation corresponds to the 9.6-ns round-trip time of the seed pulses inside the cavity. With a perfectly aligned half-wave plate (blue curve), the losses are so low that no modulation can be detected. The peak of the modulation marks the pump-energy-dependent build-up time of the amplifier. At this point, the losses in the cavity become larger than the gain of the Ti:Sapphire crystal and the signal amplitude starts to decrease. The residual light field leaves the cavity after switching the Pockels cell off. The high contrast of the modulation is an indicator for efficient seeding and low ASE.

To generate pulses at 320 nm, the two wavelengths in the amplified output are separated again by a long-pass edge filter (LP). The third harmonic of the 960 nm pulses is generated by second-harmonic generation (SHG) in an LBO crystal and subsequent sum-frequency generation in a BBO crystal. Crystal dimensions are $4 \times 4 \times 10$ mm³ for the LBO and $4 \times 4 \times 7$ mm³ for the BBO, respectively. A type-I process is used in both crystals to maximize conversion efficiency. Therefore, a dual-order wave plate is mounted between the crystals, acting as a half-wave plate for the second harmonic at 480 nm and as a full-wave plate at 960 nm. To increase the peak intensity of the pulses, a 3:1 Galilean-type telescope is used, decreasing the beam diameter to ≈ 400 μ m (FWHM). Considering the rather large walk-off in the BBO crystal, this was determined to be the optimum ratio. A dispersion prism separates the third harmonic from the residual fundamental and second-harmonic components. The relative timing of the pulses at 320 and 940 nm can be easily controlled by changing the optical path length for both wavelengths.

In order to perform triplet solvation dynamics measurements, the pulses are directed into the liquid sample mounted inside a LN₂ contact gas cryostat [6]. The light emitted by the sample is coupled into a large diameter liquid-core fibre and transferred to the grating spectrograph, where it is finally detected by an intensified CCD camera.

3 Laser system characterization

A full characterization of the laser system was performed. One of the main features of the regenerative amplifier is the flexible pulse energy ratio between the two seed wavelengths. Figure 5 shows the output energy of the amplifier for two different seed power ratios. Since the build-up time of the amplifier is pump power dependent, the width of the Pockels cell gate was tuned maximizing the pulse energy at 960 nm for each data point. Pump and output energy

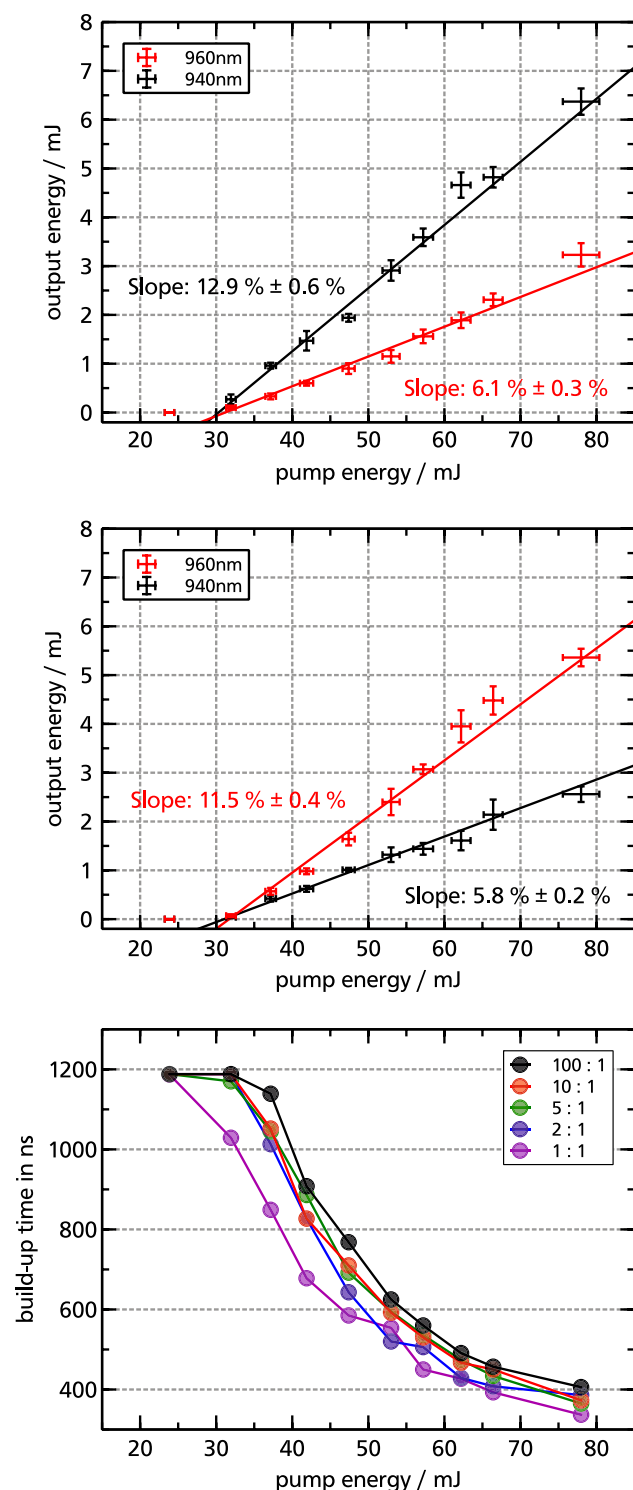


Fig. 5 Amplifier output at different seed power ratios. Top: At a seed ratio of 10:1 ($P_{960}:P_{940}$), the energy at 940 nm is still higher than at 960 nm. Middle: At a seed ratio of 100:1 ($P_{960}:P_{940}$), the slope efficiency for 960 nm is larger than for 940 nm. The required seed power at 940 nm is very low at just 0.5 mW. The overall slope efficiency is lowered, because the gain of Ti:Sapphire is lower at 960 nm than at 940 nm. Therefore, reducing the 940 nm seed power diminishes the total output energy. Bottom: Build-up time of the amplifier

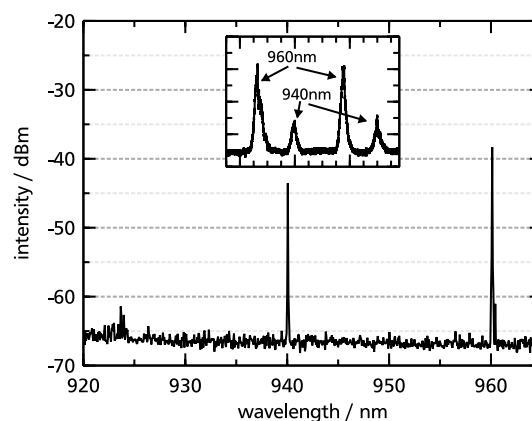


Fig. 6 Spectrum of the amplifier output for a seed ratio of 100:1 ($P_{960}:P_{940}$). The insert shows the time-averaged transmission signal of the slowly tuned FPI as described in the text. The FSR of the FPI was 1 GHz

were measured by two individual pyro-detectors (Gentec QE25SP-H-MB-DO for the pump and QE12SP-H-MT-DO for the output, respectively) over 60 s or 600 pulses in order to create statistical information. A long-term average energy (5 h) was measured to be $3.5 \text{ mJ} \pm 0.5 \text{ mJ}$ at a pump energy of 60 mJ for the 960 nm pulses. Similar energy stability was observed at 940 nm. The relatively high standard deviation is caused by the build-up time fluctuations of the amplifier combined with the fixed Pockels cell gate of the amplifier: As shown in Fig. 5, the build-up time of the amplifier does not reach a constant value for the pump energies employed. Thus, pump energy fluctuations are translated into output energy fluctuations since the amplifier pulse is always extracted at a fixed time by switching off the Pockels cell.

Pulse energies of up to 1 mJ at 320 nm were achieved with 3.5 mJ in the fundamental corresponding to a maximum conversion efficiency of 27.6 % for third-harmonic generation. The long-term (5 h) average output energy at 320 nm was measured to be $0.73 \text{ mJ} \pm 0.25 \text{ mJ}$. The amplifier output beam shows very low astigmatism and is nearly Gaussian with a $1/e^2$ -width of 2 mm and good collimation [see Fig. 4 (right)].

An optical spectrum analyser (Yokogawa AQ 6373) was used to measure the suppression of the amplified spontaneous emission (see Fig. 6). The background is suppressed by at least -18 dB at 80 mJ pump energy and can be easily filtered from the output. ASE in spectral regions closer to the gain peak is negligible.

At a measured pulse duration of $(6.46 \pm 0.09) \text{ ns}$, the Fourier-limited spectral width for a Gaussian pulse shape amounts to $(68.27 \pm 0.95) \text{ MHz}$. The spectral width of the pulses was measured by slowly scanning a high finesse

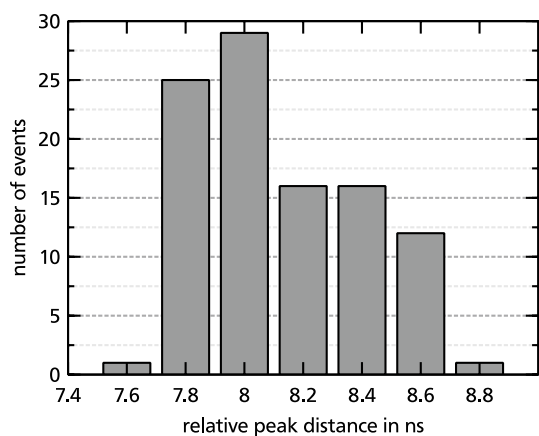


Fig. 7 Histogram of the relative peak distance between the two wavelengths for an optical delay of 2.41 m

($F = 300$) Fabry–Pérot interferometer (FPI) with a free spectral range of 1 GHz and integrating the transmission signal with a boxcar integrator. By fitting an Airy function to the data, the average spectral bandwidth of the pulses was determined to (67.84 ± 2.34) MHz for 940 nm and (67.66 ± 0.34) MHz for 960 nm. This is in agreement with the Fourier transform limit. Thus, the amplifier generates Fourier-transform-limited pulses also explaining the high conversion efficiency into the third harmonic.

The timing jitter between the two wavelengths was measured by separating the pulses with a long-pass edge filter, delaying the 960 nm pulse by an optical path of 2.41 m and then recording both pulses simultaneously with a fast APD. The temporal distance between both wavelengths was determined from the relative position of the two peaks in the APD signal. A histogram of the relative peak positions for 100 consecutive pulses with a standard deviation of 281 ps is shown in Fig. 7. The accuracy of this measurement is again limited by build-up time fluctuations. Pulse duration at 320 nm (≈ 2.4 ns) is nearly ten times longer. The overall mechanical reliability of the laser system is excellent. Adjustment intervals are several weeks for the amplifier and THG and several months for the two seed lasers, respectively.

4 Conclusion

In summary, we have demonstrated a ns regenerative Ti:Sapphire amplifier with Fourier-transform-limited pulses and excellent beam quality far off the gain peak at 940 and 960 nm. In combination with our earlier work, we have shown that almost arbitrary combinations of two wavelengths can be simultaneously amplified in our set-up. The relative pulse energy can be adjusted by simple control of the seed power at the respective wavelengths. In principle, it should be possible to extend this scheme to more than two wavelengths. Timing between the pulses can be controlled by an optical delay line. Furthermore, we have demonstrated efficient nonlinear frequency conversion. Mechanical stability was excellent. Therefore, this laser system can be applied to a variety of pump-probe studies in the ns regime in molecular and atomic physics, lidar or applications in coherent control.

Acknowledgments The authors thank the Deutsche Forschungsgemeinschaft (DFG) for funding through the Research Unit FOR 1583.

References

1. V. Stert, W. Radloff, C.P. Schulz, I.V. Hertel, Ultrafast photoelectron spectroscopy: femtosecond pump-probe coincidence detection of ammonia cluster ions and electrons. *Eur. Phys. J. D At. Mol. Opt. Plasma Phys.* **5**(1), 97–106 (1999)
2. K. Wendt, N. Trautmann, B.A. Bushaw, Resonant laser ionization mass spectrometry: An alternative to AMS? *Nucl. Instrum. Methods Phys. Res. B* **172**(1–4), 162–169 (2000). (**8th International Conference on Accelerator Mass Spectrometry**)
3. G.A. Rines, H.H. Zenzie, R.A. Schwarz, Y. Isyanova, P.F. Moulton, Nonlinear conversion of Ti:sapphire laser wavelengths. *IEEE J. Sel. Top. Quantum Electron.* **1**(1), 50–57 (1995)
4. C. Tian, T. Walther, R. Nicolaescu, X.J. Pan, Y. Liao, E.S. Fry, Synchronous, dual-wavelength, injection-seeded amplification of 5-ns pulses in a flash-lamp-pumped Ti: Sapphire laser. *Opt. Lett.* **24**(21), 1496–1498 (1999)
5. Ranko Richert, Triplet state solvation dynamics: basics and applications. *J. Chem. Phys.* **113**(19), 8404 (2000)
6. D. Sauer, B. Schuster, M. Rosenstihl, S. Schneider, V. Talluto, T. Walther, T. Blochowicz, B. Stühn, M. Vogel, Dynamics of water–alcohol mixtures: insights from nuclear magnetic resonance, broadband dielectric spectroscopy, and triplet solvation dynamics. *J. Chem. Phys.* **140**(11), 114503 (2014)